Global Topology & Stability and Local Structure & Dynamics in a Synthetic Spin-Labeled Four-Helix Bundle Protein†

Brian R. Gibney,‡ Jonas S. Johansson,‡,§ Francesc Rabanal,‡ Jack J. Skalicky,|| A. Joshua Wand,|| and P. Leslie Dutton*,‡

Johnson Research Foundation, Department of Biochemistry and Biophysics, and Department of Anesthesia, University of Pennsylvania, Philadelphia, Pennsylvania 19104, and Departments of Chemistry, Biological Sciences, and Biophysical Sciences and Center for Structural Biology, State University of New York, Buffalo, New York 14260

Received July 23, 1996; Revised Manuscript Received November 20, 1996⊗

ABSTRACT: A maleimide nitroxide spin-label (MAL-6) linked to a cysteine in the hydrophobic core and a coproporphyrin I (CP) appended on the N-terminus of a synthetic helix−loop−helix peptide ($[\alpha_2]$) have been used to examine the designed self-association of a four-helix bundle ($[\alpha_2]_2$), focusing on the bundle topology and stability and the rotational dynamics of the spin-label. Gel-permeation chromatography demonstrated that the $[\alpha_2]$ peptide and the peptide modified with a spin-label ([MAL-6-α_2]), a coproporphyrin ([CP-α_2]) and a coproporphyrin plus a spin-label ([CP-MAL-6-α_2]) self-associate into four helix bundles in solution as designed. Circular dichroism (CD) spectra prove that all these peptides are highly α-helical, confirmed for $[\alpha_2]_2$ by Fourier transform infrared (FTIR) spectroscopic analysis. Electron spin resonance (ESR) spectra of the two attached maleimide spin-labels in [MAL-6-α_2]$_2$ shows their effective rotational correlation time (τ_c) is 7.3 ± 0.5 ns, consistent with that expected for the tumbling of the four helix bundle itself, indicating the labels are immobilized. The ESR spectra were also unaltered by aqueous-phase paramagnetic ions, Ni(II), demonstrating all of the spin-labels are buried within the hydrophobic core. The lack of spin−spin interaction between the buried, immobilized spin-labels indicates they are remote (>15 Å) from each other, indicating an antiparallel topology of the monomers in [MAL-6-α_2]$_2$. The parent $[\alpha_2]_2$ and the modified [MAL-6-α_2]$_2$ and [CP-α_2]$_2$ peptides are highly stable (ΔG^{H_2O} ≈ 25 kcal/mol) as investigated by guanidine hydrochloride denaturation curves monitored by ESR and CD spectroscopies. Guanidine hydrochloride denaturation leads to a shorter correlation time of the spin-label, τ_c < 1 ns, approaching that of an unrestricted spin-label in solution. In contrast, trifluoroethanol caused dissociation of [MAL-6-α_2]$_2$ to yield two [MAL-6-α_2] monomers with retention of secondary structure and changed the τ_c to 2.5 ± 0.5 ns, indicating that a significant degree of motional restriction is imposed on the spin-label by the secondary structure. The coproporphyrin probes covalently attached to the N-termini of [CP-α_2]$_2$ and [CP-MAL-6-α_2]$_2$ provided evidence that the helical monomers of both were in a parallel orientation, in contrast to the antiparallel orientation determined for [MAL-6-α_2]$_2$. Consequently, the ESR spectra of [MAL-6-α_2]$_2$ and [CP-MAL-6-α_2]$_2$ reveal major structural differences in the local vicinity of the spin-labels due to the topological difference between these two bundles. The ESR spectra of [CP-MAL-6-α_2]$_2$ contains two distinct nitroxide populations, indicating that one spin-label remains buried in the hydrophobic core and the other is excluded to solvent in this parallel topology. Alleviation of the steric interactions causing one spin-label in [CP-MAL-6-α_2]$_2$ to be solvent-exposed by addition of [CP-α_2]$_2$ results in formation of the heterodimeric [CP-α_2]/[CP-MAL-6-α_2], as evidenced by insertion of all the spin-labels into hydrophobic cores. The changes in global topology and local structure as evidenced by this pair of spectral probes have relatively minor effects on the course of guanidine denaturation of these bundles.

Our approach to the study of complex natural oxidoreductases is to design and synthesize minimalist structures that assemble the component peptides with incorporated redox cofactors. The extended goal is to generate molecular *maquettes*, functional synthetic versions of complex native enzymes considerably simplified because of the removal of protein domains which may be present in enzymes for purposes other than catalysis. Our success with the ligation of up to four hemes within a tetra-α-helical bundle as a maquette for the cytochrome bc_1 complex (Robertson et al., 1994; Choma et al., 1994; Kalsbeck et al., 1996), the covalent attachment of a pendant porphyrin dimer as the principal component of a maquette for the photosynthetic reaction center (Rabanal et al., 1996a,b), and the incorporation of an iron−sulfur cluster to the loop region for a ferredoxin maquette (Gibney et al., 1995, 1996) poses questions as to the stability and dynamics of the chosen tetra-α-helical

†This work was supported by the National Institutes of Health (Grants GM27309 and GM41048 to P.L.D. and GM 35940 to A.J.W.). B.R.G. and J.J.S. gratefully acknowledge receipt of postdoctoral fellowships from the NIH (Grants GM17816 and GM18121, respectively). J.S.J. was supported in part by a Foundation for Anesthesia Education and Research Young Investigator Award. F.R. was supported by a postdoctoral fellowship from the European Molecular Biology Organization. The infrared spectrometer is supported by the NIH (GM 48130).

‡ Johnson Research Foundation, Department of Biochemistry and Biophysics, University of Pennsylvania.

§ Department of Anesthesia, University of Pennsylvania.

|| State University of New York.

⊗ Abstract published in *Advance ACS Abstracts,* February 15, 1997.

S0006-2960(96)01822-3 CCC: $14.00

bundle scaffold and to the effects of subsequent cofactor incorporation. The first stage toward the successful manipulation of any designed protein with the aim of establishing catalytic fitness is acquisition of the requisite protein stability for construction of a singular protein structure.

While quantitative descriptions of the factors governing α-helical (Chakrabartty et al., 1994; O'Neil & DeGrado, 1990; Zhao et al., 1993) and β-sheet (Smith & Regan, 1995) peptide stability are becoming available, the factors that specify unique structures (DeGrado et al., 1989; Betz et al., 1993; Struthers et al., 1996) are much less well delineated and the intricacies of protein−cofactor interactions within synthetic peptides are virtually unstudied (Bryson et al., 1995). Research to elucidate the factors governing side-chain packing specificity is making use of genetic algorithms (Desjarlais & Handel, 1995), protein simulated evolution (Hellinga & Richards, 1994), engineered metal binding sites (Ghadiri & Choi, 1990; Regan & Clarke, 1990; Handel et al., 1993; Wade et al., 1993), and combinatorial libraries (Kamtekar et al., 1993) to redesign/stabilize unique hydrophobic cores within four helix bundle proteins. However, these efforts to redesign peptides toward nativelike proteins have suffered from a paucity of analytical methods that have been applied to reveal the physicochemical nature of the hydrophobic cores and the overall topologies in the native state.

In our prototype H10H24 series of heme maquettes, the reliance on leucine side chains to drive four helix bundle formation from a pair of di-α-helical monomers resulted in a nonnative hydrophobic core. The existence of two isoenergetic rotamers of leucine within an α-helical secondary structure (McGregor et al., 1987; Dunback & Karplus, 1994) results in uncertainties in the modeling of the designed structure. This uncertainty is compounded by the additional topological complexity resulting from the construction of four helix bundle proteins from a pair of α_2 monomers or from four α monomers without specific interactions designed within the hydrophobic core. In fact, a mixture of interconverting topologies might not be unexpected in such simple structures incorporating minimal hydrophobic cores. So far, in the case of the H10H24 series evidence for a parallel arrangement of di-α-helical monomers came initially from arguments based on electrostatic interactions between the four bound hemes but then more directly from introduction of a coproporphyrin spectral probe (Rabanal et al., 1996a).

The electron spin resonance (ESR)[1] spin-labeling technique is a highly sensitive method for examining protein structure requiring minimal sample quantities (Morrisett & Broomfield, 1971; Berliner, 1972; Schneider & Freed, 1989; Millhauser et al., 1995; Mchaourab et al., 1996). It has proven a powerful method for mapping membrane spanning regions of proteins (Snel & Marsh, 1993; Snel et al., 1994), determining peptide−receptor interactions (Liu et al., 1994), evaluating distances in metalloproteins (Voss et al. 1995a,b), investigating protein conformational changes (Farahbakhsh et al., 1993; Resek et al., 1993) and denaturation (Klug et al., 1995), elucidating protein structural motifs (Miich et al., 1992; Fiori & Millhauser, 1995; Smythe et al., 1995) and determining aggregation states (Mchaourab et al., 1993). Advances in site-directed spin-labeling (Hubbell & Altenbach, 1994) in which solid-phase synthesis is used to introduce cysteine labeling sites at desired locations, illustrated in Scheme 1, has greatly expanded the applicability of the spin-labeling technique. In the present work, we make use of the ESR resonances to provide the means to assess not only global topology but also variations in structural dynamics of the immediate environment of the nitroxide spin-label.

Scheme 1

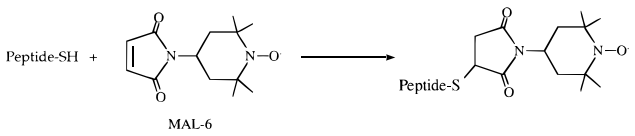

In this paper, we describe the synthesis and characterization of a helix−loop−helix peptide, α_2, designed to self-associate to form a four helix bundle, $[\alpha_2]_2$, as was observed with our earlier heme protein maquettes (Robertson et al., 1994; Rabanal et al., 1996a−c). The α_2 peptide was further equipped with a nitroxide spin-label probe (MAL-6) attached to a cysteine at position 41 designed to probe the hydrophobic core and the topology of the dimeric bundle, [MAL-6-α_2]$_2$. A remotely placed external pendant coproporphyrin I (CP) was also attached to α_2 as a spectral probe, [CP-α_2]. ESR resonances of the spin-labels in the [MAL-6-α_2]$_2$ and [CP-MAL-6-α_2]$_2$ bundles reveal not only their positions in the structures but also the individual dynamics of their immediate environments.

EXPERIMENTAL PROCEDURES

Chemicals and Solvents. *N*-(2,2,6,6-Tetramethylpiperidin-4-yl-1-oxyl)maleimide was purchased from Molecular Probes (Eugene, OR). Coproporphyrin I dihydrochloride, diisopropylcarbodiimide, *N*,*N*-diisopropylethylamine, trifluoroethanol, and trifluoroacetic acid were obtained from Aldrich Chemical Co. (Milwaukee, WI). Ethanedithiol was purchased from Fluka (Ronkonkoma, NY). Guanidine hydrochloride (8 M) was used as received from Pierce (Rockford, IL). Fmoc-protected amino acid perfluorophenyl esters were purchased from PerSeptive Biosystems (Framingham, MA) with the exception of Fmoc-L-Arg(Pmc)-OPfp, which was obtained from Bachem (King of Prussia, PA). NovaSyn PR-500 resin was purchased from Calbiochem−Novabiochem (La Jolla, CA). All other chemicals and solvents were reagent grade.

Peptide Sequences. [α_2] has the sequence Ac-L KKL-REEA LKLLEEF KKLLEEA LKLLE GGGGGGGG EL-WKL CEELLKK FEELLKL AEERLKK L-CONH$_2$. [CP-α_2] has the same sequence with coproporphyrin I replacing the N-terminal acetyl group.

[1] Abbreviations: MAL-6, *N*-(2,2,6,6-tetramethylpiperidin-4-yl-1-oxyl)maleimide; [α_2], helix−loop−helix peptide; [MAL-6-α_2], helix−loop−helix with spin-label attached; [CP-α_2], helix−loop−helix with coproporphyrin I covalently bound; [CP-MAL-6-α_2], helix−loop−helix with both coproporphyrin I and spin-label covalently bound; FTIR, Fourier transform infrared spectroscopy; CD, circular dichroism; Θ_{222}, ellipticity at 222 nm; ESR, electron spin resonance; τ_c, rotational correlation time; TFE, trifluroethanol; Gdn·HCl, guanidine hydrochloride; Fmoc, 9-fluorenylmethoxycarbonyl; OPfp, pentafluorophenyl ester; ^{t}Boc, *tert*-butoxycarbonyl; Trt, trityl or triphenylmethyl; O^{t}Bu, *tert*-butyl ester; Pmc, 2,2,5,7,8-pentamethylchroman-6-sulfonyl; HOBt, 1-hydroxybenzotriazole; HPLC, high-performance liquid chromatography; NMR, nuclear magnetic resonance; FID, free induction decay; DSS, 2,2-dimethyl-2-silapentane-5-sulfonic acid; COSY, correlation spectroscopy; ΔG_{unf}, difference in Gibbs free energy between denatured and folded protein; DMF, *N*,*N*-dimethylformamide.

Peptide Synthesis. The peptides were synthesized on a continuous-flow Milligen 9050 solid-phase synthesizer using standard Fmoc/^{t}Bu protection strategy with NovaSyn PR-500 resin at 0.2-mmol scale. Extended coupling cycles (60 min) were employed to enhance the yield of reaction. The side-chain protecting groups used are as follows: Lys (^{t}Boc), Glu (O^{t}Bu), Cys (Trt), and Arg (Pmc). The N-terminus was either acetylated [1:1 (v/v) acetic anhydride:pyridine for 30 min] for [α_2] and [MAL-6-α_2] or attached to coproporphyrin I for [CP-α_2] and [CP-MAL-6-α_2] as described below. The peptides were cleaved from the resin and simultaneously deprotected using 90:8:2 trifluoroacetic acid:ethanedithiol: water for 2 h. Crude peptides were precipitated and triturated with cold ether, dissolved in water (0.1% TFA), lyophilized, and purified to homogeneity by reversed-phase C_{18} HPLC using aqueous acetonitrile gradients containing 0.1% (v/v) TFA. The resulting peptide identities were confirmed with laser desorption mass spectrometry. The synthesis yielded approximately 25 mg of purified [α_2] peptide (3% yield based on resin). Coproporphyrin I was attached to the N-terminus of the peptide on a small fraction of the resin (150 mg) using a 5-fold excess of porphyrin dihydrochloride, diisopropylcarbodiimide, *N*,*N*-diisopropylethylamine, and 1-hydroxybenzotriazole. After 5 hours, the resin was thoroughly washed with DMF, trifluoroethanol, and CH_2Cl_2 and dried before cleavage and purification as described above. This synthesis provided roughly 2 mg of HPLC-pure [CP-α_2] ($\approx$1% based on resin), which could then be converted to [CP-MAL-6-α_2]. The purified peptides were stored as lyophilized powders in a -20 °C freezer prior to spin-label addition to avoid disulfide formation.

Solution Molecular Weight Determination. Size-exclusion chromatography was performed on a Beckman System Gold HPLC system with a diode-array detector using a Supelco Sigmachrom GFC-100 column (300 × 7.5 mm) eluted with aqueous buffer (10 mM KP_i and 100 mM KCl, pH 8.0). The column was standardized using aprotinin (6.5 kDa), horse heart cytochrome *c* (12.1 kDa), chymotrypsinogen (25.0 kDa), ovalbumin (43.0 kDa), and bovine serum albumin (67.0 kDa).

Label Attachment. The unique cysteines of HPLC-purified α_2 and [CP-α_2] were labeled with *N*-(2,2,6,6-tetramethylpiperidin-4-yl-1-oxyl)maleimide (MAL-6) by incubating 10 equiv of spin-label in 10−20% acetonitrile in 30 mM KP_i and 120 mM KCl, pH 7.0, with 1 equiv of peptide at 4 °C for 24 h with gentle stirring (Singh et al., 1995). Prior to the reaction, the thiol content of α_2 was confirmed using Ellman's reagent; no significant disulfide formation was detected. The reaction mixture was subsequently lyophilized and resuspended in H_2O (0.1% TFA) prior to HPLC purification. HPLC revealed the presence of four reaction products (unreacted peptide, spin-labeled peptide, disulfide-dimerized peptide, and an ESR-silent maleimide labeled peptide) which were collected and identified by mass spectrometry and ESR spectroscopy. The calculated yield of spin-labeling after HPLC purification of MAL-6-α_2 was 19% (based on peptide).

ESR Spectroscopy. Electron spin resonance (ESR) was performed using a Bruker ESP300E spectrometer operating at X-band frequencies. Frequency was measured by a Hewlett-Packard 5350B frequency counter. Samples, approximately 5-μL volume, were sealed in Pyrex capillary tubes (0.8-mm i.d.) and placed into 4-mm i.d. quartz tubes for measurement. ESR parameters, unless otherwise noted, are as follows: sample temperature, 298 K; microwave frequency, 9.449 GHz; microwave power, 10 mW; modulation frequency, 100 kHz; modulation amplitude, 4 G; time constant, 82 ms; scans, 3. The ESR spectra of motionally restricted nitroxide spin-labels ($\tau_c > 1$ ns) were fit to a diffusional coefficient with the programs LLBL, ESRLL, and TDLL (Schneider & Freed, 1989) using a Brownian diffusion model. The programs were compiled using Microsoft Fortran workstation. The MAL-6 parameters used in the simulations were as follows: $g_x = 2.0090$, $g_y = 2.0060$, $g_z = 2.0024$, $A_x = 6.8$ G, $A_y = 6.2$ G, and $A_z = 34.3$ G (Lassman et al., 1973). The truncation parameters used for the simulations were $L^e_{max} = 10$, $L^o_{max} = 8$, $K_{max} = 6$, $M_{max} = 2$, and $p^I = 2$. The number of Lanczos steps was 50.

Circular Dichroism Spectropolarimetry. CD spectra were recorded on an Aviv 62DS spectropolarimeter using rectangular quartz cells of 0.2- and 1.0-cm path length. Thermal control was maintained by a thermoelectric module with a Neslab CFT-33 refrigerated recirculating water bath as a heat sink. Peptide concentrations were between 5 and 10 μM as determined spectrophotometrically using $\epsilon_{280} = 5600$ M^{-1} cm^{-1} for Trp.

UV−Vis Spectroscopy. UV−Vis spectra were recorded on a Perkin-Elmer Lambda 2 spectrophotometer using quartz cells of 0.2- and 1.0-cm path length. Peptide concentrations were between 3 and 5 μM as determined spectrophotometrically using $\epsilon_{394} = 2 \times 10^5$ M^{-1} cm^{-1} for the coproporphyrin monomer.

Denaturation Studies. Peptide denaturation curves were fit to a dimer folded to monomer unfolded equilibrium using a nonlinear least-squares routine in KaleidaGraph (Abelbeck Software)

$$\text{fraction folded} = 1 - (K_{unf}/4P)[(1 + 8P/K_{unf})^{1/2} - 1]$$

where P is the molar concentration of total monomeric protein, $K_{unf} = \exp(-\Delta G_{unf}/RT)$, and $\Delta G_{unf} = \Delta G^{H_2O} + m$[Gdn·HCl], where m is the cosolvation term, which is a measure of the cooperativity of the transition, and [Gdn·HCl] is the molar concentration of denaturant (Pace, 1986; Mok et al., 1996).

Infrared Spectroscopy. Fourier transform infrared spectra were recorded on a Bruker IFS 66 FTIR spectrometer equipped with a Globar source, a KBr beam splitter, a mercury−cadmium−telluride detector, and an attenuated total reflectance cell (Graseby Specac, Fairfield, CT).

NMR Studies. NMR experiments were performed on a Varian INOVA-600 spectrometer. One-dimensional spectra were acquired with 8192 complex points using a spectral width of 7200 Hz/FID. The H10H24 and $[\alpha_2]_2$ peptide samples were prepared at 500 μM monomer concentration (250 μM four helix bundle) in 20 mM phosphate (pH 7.25), 50 mM KCl, and 8% D_2O. The $[\alpha_2]_2$ protein solution contained 1 mM dithiothreitol. Proton chemical shifts were referenced to an external sample of DSS at 0.00 ppm. The NMR data were processed on a SGI Crimson computer using FELIX95 software (Biosym Technologies, San Diego, CA).

RESULTS

Design of α_2. The current peptide design is based on our prototype H10H24 series of heme protein maquettes (Rob-

Table 1: Peptide Characterization

peptide	molecular weight: monomer mass	molecular weight: gel permeation, aqueous	molecular weight: gel permeation, 50% TFE	molar ellipticity (deg cm^2 dmol^{-1})	% α-helix	$[Gdn\cdot HCl]_{1/2}$	ΔG^{H_2O} (kcal mol^{-1})	m (kcal mol^{-1} M^{-1})
$[\alpha_2]_2$	7120	19000	7500	24600	77	6.7	25.7	2.7
[MAL-6-α_2]$_2$	7372	19600	7800	22000	69	6.7	25.2	2.7
[CP-α_2]$_2$	7767	20100	8000	22800	71	7.0	24.9	2.5
[CP-MAL-6-α_2]$_2$	8019	21400	8300	22000	69	6.7	25.9	2.6

ertson et al., 1994), a four helix bundle which binds 1−4 hemes that is in turn based on insights drawn from the natural cytochrome *bc*$_1$ complex (Trumpower, 1990; Ding et al., 1995) and the minimalist synthetic design of $[\alpha_2]_2$ (Ho & DeGrado, 1987). The N-terminal Cys−Cys linkage of the earlier H10H24 design, certain to interfere with spin-label attachment to a Cys elsewhere, was replaced by an amide bond, resulting in a 62 amino acid helix−loop−helix monomer, α_2, with concomitant reorientation of the helix dipoles in the α_2 monomer from parallel to antiparallel. The heme binding histidines in coiled-coil *a* positions of H10H24 were replaced at three of four analogous positions (8, 22, and 54) by alanines, chosen for their high helical propensities (O'Neil & DeGrado, 1990) and minimal side-chain volume, and by a cysteine at position 41 for the covalent attachment of a spin-label. The maleimide spin-label was selected for its rigid linker which is preferable for reporting peptide rotational freedom. Thus, the resulting helix−loop−helix monomer includes a hydrophobic core analogous to that of H10H24 minus the four histidines but with the spin-label. In addition, the N-terminal amine of the helix−loop−helix provided a site for attachment of the coproporphyrin probe remote from the spin-label.

Gel-Permeation Chromatography. The designed dimeric aggregation state of each of the peptides was evaluated using gel-permeation chromatography. The parent peptide, $[\alpha_2]_2$, when dissolved in degassed aqueous buffer (10 mM KP_i, and 100 mM KCl, pH 7.0) eluted with an apparent molecular mass of 19.0 kDa (14.1 kDa calculated for the four helix bundle) based on column standardization with globular proteins. This peptide coeluted with H10H24, a known four helix bundle, indicating that the related proteins have similar hydrodynamic radii. The spin-label-, coproporphyrin-, and spin-label/coproporphyrin-containing peptides eluted at positions consistent with four helix bundle aggregation states as given in Table 1. The table shows that when eluted in the presence of 50% (v/v) trifluoroethanol, which is known to disrupt hydrophobic interactions between individual helices, an apparent molecular mass of 7.5 kDa is obtained, consistent with dissociation of the dimeric $[\alpha_2]_2$ into monomeric $[\alpha_2]$ helical peptides.

Circular Dichroism Studies. Figure 2 shows that $[\alpha_2]_2$ in aqueous buffer (10 mM KP_i and 100 mM KCl, pH 7.0) has a CD spectrum typical of highly α-helical peptides with minima at 208 and 222 nm (Chen et al., 1974). The figure also assesses the possible perturbations in the structure of $[\alpha_2]_2$ upon incorporation of the spin-label and the pendant coproporphyrin. These spectra clearly demonstrate that addition of either or both probes to the parent peptide results in no significant alteration in the secondary structure of the parent peptide. In aqueous buffer, the $\Theta_{222}/\Theta_{208}$ ratios, ≥ 1.0, are diagnostic of coiled-coil structures (Zhou et al., 1992; Graddis et al., 1993). Introduction of trifluoroethanol (>4 M) causes the ratios of $\Theta_{222}/\Theta_{208}$ to decrease to ≈0.95, approaching the value of 0.90 (Lau et al., 1984; Dill et al., 1995) considered representative of extended or monomeric helices consistent with the gel-filtration data above.

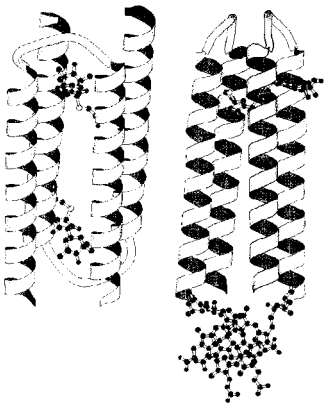

FIGURE 1: Working models of [MAL-6-α_2]$_2$ and [CP-MAL-6-α_2]$_2$ with topologies consistent with the experimental data to be presented.

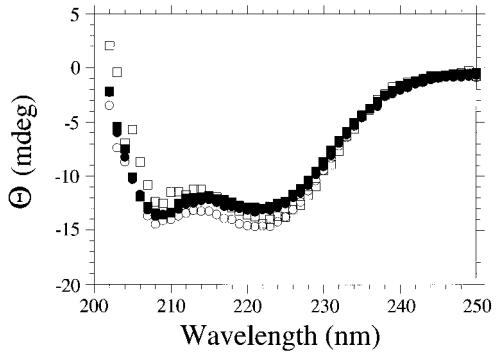

FIGURE 2: Circular dichroism spectra of peptides $[\alpha_2]_2$ (□), [MAL-6-α_2]$_2$ (○), [CP-α_2]$_2$ (■), and [CP-MAL-6-α_2]$_2$ (●) recorded at 25 °C in 20 mM sodium phosphate and 130 mM NaCl buffer, pH 7.0. Peptide concentrations were 9.5 μM as determined spectrophotometrically using Trp (ϵ_{280} = 5600 M^{-1} cm^{-1}).

Infrared Spectroscopy. The FTIR spectrum of a millimolar solution of $[\alpha_2]_2$ in D_2O [10 mM KP_i and 100 mM KCl, pH 8.0 (uncorrected)] displays a strong absorbance at 1653 cm^{-1} indicative of the amide I′ band of an α helix (typical range 1650−1657 cm^{-1}) corroborating the secondary structure observed by circular dichroism.

UV−Vis Spectroscopy of [CP-α_2*]*$_2$ *and [CP-MAL-6-*α_2*]*$_2$*.* In aqueous degassed buffer (10 mM KP_i and 100 mM KCl, pH 7.0) at micromolar peptide concentrations, both [CP-α_2]$_2$ and [CP-MAL-6-α_2]$_2$ display Soret maxima at 372 nm, indicative of coproporphyrin cofacial dimer formation (Rabanal et al., 1996b). Thus, the helix−loop−helix monomers, [CP-α_2] and [CP-MAL-6-α_2], within their respective dimer proteins, [CP-α_2]$_2$ and [CP-MAL-6-α_2]$_2$, clearly adopt parallel topologies. Molecular models of [CP-α_2]$_2$ in a parallel topology indicate a $S_{Cys}-S_{Cys}$ distance of ≈10 Å.

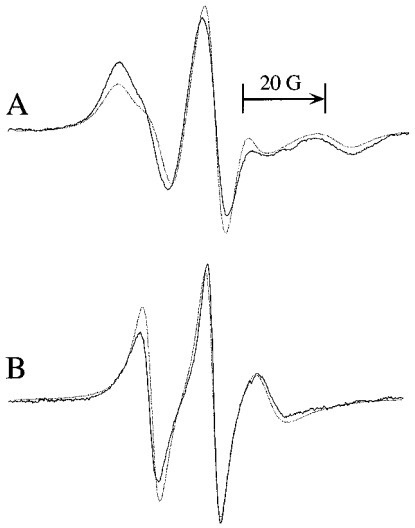

FIGURE 3: Experimental (solid line) and simulated (dotted line) ESR spectra of [MAL-6-α_2]$_2$ in aqueous buffer (A) and in 5.5 M TFE (B). Each sample contained 60 μM [MAL-6-α_2]$_2$, 20 mM sodium phosphate, and 130 mM NaCl, pH 7.0. The modulation amplitude of the 5.5 M TFE sample was 1 G.

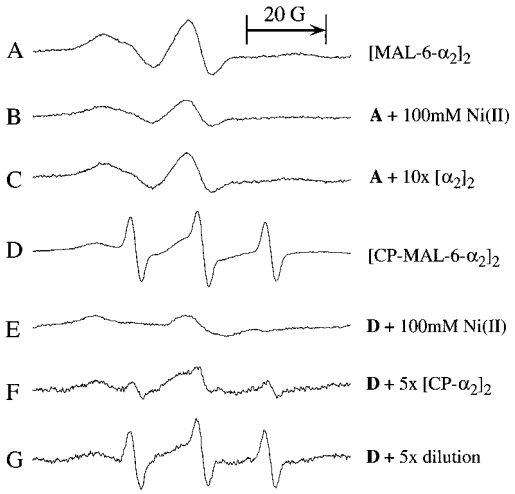

FIGURE 4: ESR spectra (9.4 GHz) of the spin-labeled peptides. ESR spectra are shown for (A) [MAL-6-α_2]$_2$ at 8 μM peptide concentration; (B) [MAL-6-α_2]$_2$ with Ni(II) (100 mM $NiCl_2$) (2× dilution relative to A), (C) [MAL-6-α_2]$_2$ with a 10-fold excess of [α_2]$_2$, (D) [CP-MAL-6-α_2]$_2$ at 4 μM concentration, (E) [CP-MAL-6-α_2]$_2$ with Ni(II) (100 mM $NiCl_2$) (2× dilution relative to D), (F) [CP-MAL-6-α_2]$_2$ with a 5-fold excess of [CP-α_2]$_2$ (5× dilution relative to D), and (G) [CP-MAL-6-α_2]$_2$ with a 5-fold excess of buffer (5× dilution relative to D).

ESR of [MAL-6-α_2]$_2$. Figure 3A shows that the spin-labeled peptide, [MAL-6-α_2]$_2$, yields an ESR spectrum indicative of a strongly immobilized nitroxide radical (Goldman et al., 1972, 1973) without predominant spin−spin interactions. The rotational correlation time, τ_c, determined by simulation (shown as dotted line) of the spectrum is 7.3 ± 0.5 ns, a time consistent with the τ_c of a spherical protein of 17.5 kDa. This compares favorably with the apparent 19.6 kDa (calculated τ_c = 8.2 ns) solution molecular mass determined by gel-permeation chromatography, indicating that the immobilized spin-label is tumbling along with the four helix bundle itself. The solvent accessibility of the spin-label was probed by dilution with Ni(II), a water-soluble paramagnetic relaxation agent, as shown in Figure 4B. The lack of alteration in the line shape or intensity of the nitroxide radical ESR spectrum in the presence of 100 mM $NiCl_2$ demonstrates that both labels are sequestered within the hydrophobic core of the protein and away from solvent. The spin-label line shapes also show no perturbation due to spin−spin interactions between the two nitroxide radicals in [MAL-6-α_2]$_2$, placing a minimal interspin separation of ≥15 Å. This observation together with the observed effective location away from solvent strongly suggests that the two halves of [MAL-6-α_2]$_2$ are arranged in an antiparallel topology as shown in Figure 1. Molecular models of this antiparallel topology suggest that it places a distance of ≈27 Å between the cysteine sulfurs of [MAL-6-α_2]$_2$. It is interesting to note that this conclusion contrasts with the parallel topology of the monomers in [CP-α_2]$_2$ and [CP-MAL-6-α_2]$_2$ deduced from the observed coproporphyrin cofacial dimer in their structures, as discussed for the UV−Vis data above. Hence, the ESR properties of the spin-labels of [CP-MAL-6-α_2]$_2$ are expected to display some differences from those of [MAL-6-α_2]$_2$.

ESR of [CP-MAL-6-α_2]$_2$. Figure 4D shows that the ESR spectrum of [CP-MAL-6-α_2]$_2$ at micromolar concentrations is, as anticipated, markedly different from that observed for [MAL-6-α_2]$_2$ (Figure 4A). The ESR of [CP-MAL-6-α_2]$_2$ was recorded at concentrations below the K_d of free coproporphyrin (20 μM) to minimize complications due to porphyrin-driven dimerization. The ESR spectrum of [CP-MAL-6-α_2]$_2$ comprises two components: a fully immobilized spin-label, as observed for [MAL-6-α_2]$_2$, and a motionally narrowed spectral component, typical of a spin-label with a high degree of rotational freedom. Subtraction of the ESR signal derived from [MAL-6-α_2]$_2$ (an immobilized spin-label) allowed deconvolution of these two components, and double integration of each indicated they comprised equivalent populations within experimental error. Furthermore, the presence of 100 mM $NiCl_2$ in samples of [CP-MAL-6-α_2]$_2$ abolished the narrowed signal of the rapidly rotating population (Figure 4E), showing that half of the spin-labels are susceptible to paramagnetic relaxation by the Ni(II) and hence are solvent-exposed. In contrast, the ESR spectra of the slowly tumbling half of the spin-label population was unaffected by the presence of Ni(II), demonstrating that this label population, like the entire population of [MAL-6-α_2]$_2$, remains shielded from solvent and rigidly localized within the hydrophobic core of the protein. Careful examination of the ESR spectra of the two populations of spin-labels in [CP-MAL-6-α_2]$_2$ failed to indicate the existence of dipolar spin coupling, indicating that they are >15 Å apart.

ESR of [CP-α_2/CP-MAL-6-α_2]. The possibility of steric interactions between the two spin-labels in the parallel [CP-MAL-6-α_2]$_2$ forcing one to become solvent-exposed was investigated by the addition of unlabeled coproporphyrin peptide, [CP-α_2]$_2$. It was expected that the [CP-MAL-6-α_2]$_2$ and [CP-α_2]$_2$ would rapidly mix to form a statistical mixture of the heterodimeric [CP-α_2/CP-MAL-6-α_2], leading to relief of the steric interaction as shown in Scheme 2. The stepwise addition of up to 5 equiv of non-spin-labeled peptide, [CP-α_2]$_2$, to [CP-MAL-6-α_2]$_2$ to shift the association equilibrium to form a dominant population of the hybrid [CP-α_2/CP-MAL-6-α_2] four helix bundle results in a gradual reduction in the intensity of the rapidly rotating component of the ESR spectrum and a corresponding increase in the slow motion component, Figure 4F. After each sample addition, spectral changes were complete and equilibrated within 1 min, indicating a prompt and facile dissociation/reassociation and

Scheme 2

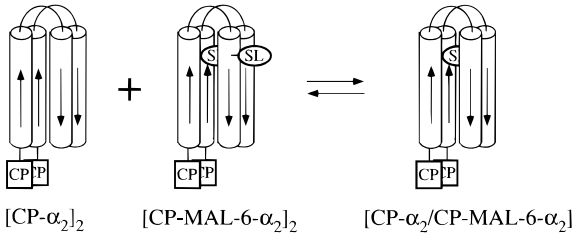

mixing of the di-α-helical monomers under these conditions. Conversion of the rapidly tumbling component to a slowly tumbling component is consistent with insertion of both spin-labels into the interior of the bundles. Control experiments, shown in Figure 4G, demonstrated no change in ESR line shape upon dilution of the sample with buffer, indicating that the changes observed are due to the production of [CP-α_2/CP-MAL-6-α_2] and not to simple dilution effects. In contrast to the [CP-MAL-6-α_2]$_2$ and [CP-α_2]$_2$ mixing experiment, addition of 10 equiv of non-spin-labeled [α_2]$_2$ to a solution of [MAL-6-α_2]$_2$ results in no alteration in the ESR line shape, Figure 4C. These observations are consistent with steric repulsions preventing the insertion of both spin-labels into the interior of the parallel [CP-MAL-6-α_2]$_2$. These data indicate that in the parallel [CP-MAL-6-α_2]$_2$ one spin-label is contained within the hydrophobic core while the tightly packed interior excludes the other, exposing it to solvent.

Trifluoroethanol Dissociation. Trifluoroethanol added at molar concentrations dissociates the spin-labeled peptide [MAL-6-α_2]$_2$ into the monomeric [MAL-6-α_2] as described above by both CD spectroscopy and gel-permeation chromatography. In contrast to the subtle changes observed in the CD spectra upon addition of trifluoroethanol, ESR spectroscopy (Figure 5) shows dramatic changes in the dynamics of the spin-label. At moderate concentrations [<20% (v/v), 2.7 M TFE], sufficient to increase the α-helical content of [MAL-6-α_2]$_2$ but not dissociate it to [MAL-6-α_2] as observed by CD, there is a subtle change in the ESR spectrum of [MAL-6-α_2]$_2$ consistent with an increase in a fast motion component. At concentrations of TFE sufficient to disrupt the coiled-coil structure of [MAL-6-α_2]$_2$ and dissociate it into [MAL-6-α_2] monomers (5.5 M, observed by CD and gel permeation), dramatic changes in the ESR spectrum were observed as it narrowed and became more intense, indicative of faster rotation of the spin-label. Simulation of the ESR spectrum of [MAL-6-α_2] in 5.5 M TFE, shown in Figure 3B, provides an effective spin-label rotational correlation time of 2.5 ± 0.5 ns, which is far from the subnanosecond time expected for a freely rotating spin-label. These data suggest that, at relatively low concentrations of TFE in which α-helix stability may be enhanced, the already immobilized spin-label remains immobilized, consistent with the four helix bundle remaining intact. However, the dissociation of the four helix bundle, at high concentrations of TFE, to yield helix−loop−helix monomers renders the buried spin-label more mobile and yet not freely tumbling.

Guanidine Hydrochloride Denaturation. Molar concentrations of guanidine hydrochloride are required to denature [α_2]$_2$, [MAL-6-α_2]$_2$, and [CP-MAL-6-α_2]$_2$ as studied by CD, ESR, and UV-vis spectroscopies. Upon addition of guanidine hydrochloride, the CD spectrum of [α_2]$_2$ loses ellipticity at Θ_{222}, consistent with denaturation to form disordered

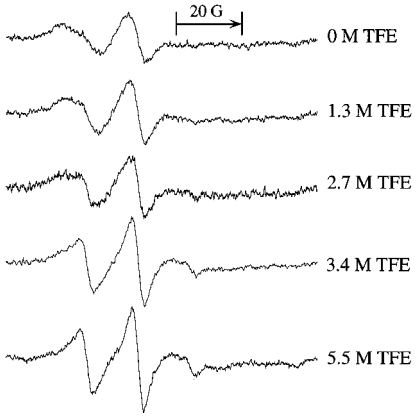

FIGURE 5: ESR spectra of [MAL-6-α_2]$_2$ in the presence of trifluoroethanol (TFE). [MAL-6-α_2]$_2$ in 0, 1.3, 2.7, 3.4, and 5.5 M trifluoroethanol. Each sample contained 5 μM [MAL-6-α_2]$_2$, 20 mM sodium phosphate, and 130 mM NaCl, pH 7.0.

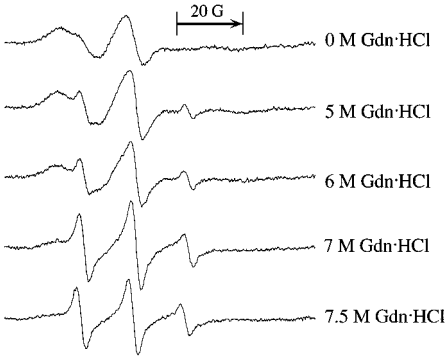

FIGURE 6: ESR spectra of [MAL-6-α_2]$_2$ upon addition of 0, 5, 6, 7, and 7.5 M guanidine hydrochloride. Each sample contained 5 μM [MAL-6-α_2]$_2$, 20 mM sodium phosphate, and 130 mM NaCl, pH 7.0.

structures with a [Gdn·HCl]$_{1/2}$ value of 6.7 M (ΔG^{H_2O} = 25.7 kcal mol^{-1}; m = 2.7 kcal mol^{-1} M^{-1}). Monitoring the loss of native secondary structure of [MAL-6-α_2]$_2$ by the decrease in Θ_{222} in the CD spectrum yields a similar [Gdn·HCl]$_{1/2}$ value of 6.7 M (ΔG^{H_2O} = 25.2 kcal mol^{-1}; m = 2.7 kcal mol^{-1} M^{-1}), indicating that attachment of the spin-label causes only minor perturbations in bundle stability. When the spin-label itself is monitored by ESR (Figure 6), the increasing guanidine concentration causes the spectral line shape of [MAL-6-α_2]$_2$ to narrow and increase in peak height, consistent with an increase in average motion of the spin-label with respect to its local environment (Berliner, 1972). Due to slight overmodulation of the ESR spectrum of the spin-label in 7.5 M [Gdn·HCl], only an upper limit of the rotational correlation time can be estimated (at <1 ns), which is significantly faster than that observed in 5.5 M TFE, confirming that the secondary structure present in the TFE-produced [MAL-6-α_2] monomers acts to partially restrict spin-label motion. Monitoring the loss of the native structure by increase in the mobility of the spin-label provides a [Gdn·HCl]$_{1/2}$ value of 6.5 M (ΔG^{H_2O} = 24.9 kcal mol^{-1}; m = 2.6 kcal mol^{-1} M^{-1}) consistent with the CD results. Guanidine hydrochloride denaturation of the peptide, monitored by CD and ESR spectroscopies, indicates that disruption of the secondary and tertiary structures of the bundle releases the spin-label further from its immobilized state. In the fully denatured state, the rapid rotational correlation time is indicative of a rapidly rotating spin-label relatively unhindered by attachment to the peptide.

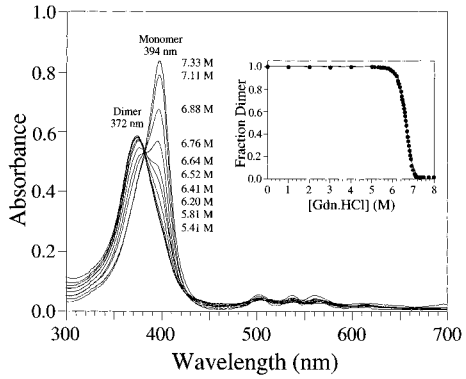

FIGURE 7: Coproporpyrin dimer reassembly monitored by UV−visible spectroscopy. At high concentrations of guanidine hydrochloride the monomeric porphyrin spectrum (λ_{max} 394 nm) predominates, indicating the peptide is fully unfolded. Dilution of the denaturant results in an increase in the the dimeric porphyrin spectrum (λ_{max} 372 nm). The inset shows the absorbance ratio (A_{394}/A_{372}) of the porphyrin dimer/monomer intensity as a function of guanidine hydrochloride.

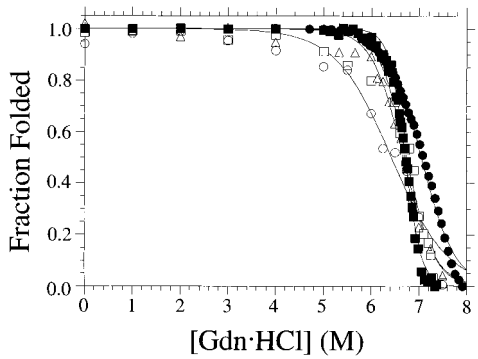

FIGURE 8: Protein denaturation curves of each peptide monitored by various techniques. The peptides $[\alpha_2]_2$ (□) and [MAL-6-α_2]$_2$ (△) as evaluated by circular dichroism spectropolarimetry. The unfolding of [MAL-6-α_2]$_2$ (○) as determined by ESR spectroscopy. The refolding of the porphyrin-containing peptides, [CP-α_2]$_2$ (●) and [CP-MAL-6-α_2]$_2$ (■), as monitored by UV−vis spectroscopy. All spectra were recorded at 25 °C in 10 mM potassium phosphate and 100 mM KCl buffer, pH 7.0. Peptide concentrations were 3−10 μM as determined spectrophotometrically using Trp ($\epsilon_{280} = 5600$ M^{-1} cm^{-1}) or coproporphyrin monomer ($\epsilon_{394} = 2 \times 10^5$ M^{-1} cm^{-1}). The parameters used to fit each experimental curve are given in the text.

Renaturation of [CP-α_2]$_2$ and [CP-MAL-6-α_2]$_2$ from the guanidine hydrochloride denatured state was monitored by UV−visible spectroscopy. When [CP-α_2]$_2$ and [CP-MAL-6-α_2]$_2$ are dissolved in 8 M guanidine hydrochloride, the UV−visible spectra display Soret maxima at 394 nm indicative of a monomeric coproporphyrin I. Figure 7 illustrates that addition of aqueous buffer to [CP-MAL-6-α_2]$_2$ dissolved in 8 M guanidine hydrochloride results in a shift of the Soret from 394 to 372 nm due to exiton coupling, indicating porphyrin dimerization (Rabanal et al., 1996a). Monitoring the peptide reassembly by coproporphyrin dimerization yields a $[Gdn{\cdot}HCl]_{1/2}$ value of 7.0 M ($\Delta G^{H_2O} = 24.9$ kcal mol^{-1}; $m = 2.5$ kcal mol^{-1} M^{-1}) for [CP-α_2]$_2$, as shown in Figure 8, and $[Gdn{\cdot}HCl]_{1/2}$ value of 6.7 M ($\Delta G^{H_2O} = 25.9$ kcal mol^{-1}; $m = 2.6$ kcal mol^{-1} M^{-1}) for [CP-MAL-6-α_2]$_2$. These data indicate that addition of the pendant N-terminal coproporphyrin and its tendency to form a cofacial dimer results in only relatively minor alteration of the bundle stability; as such, it provides a ready probe of four helix bundle disassembly.

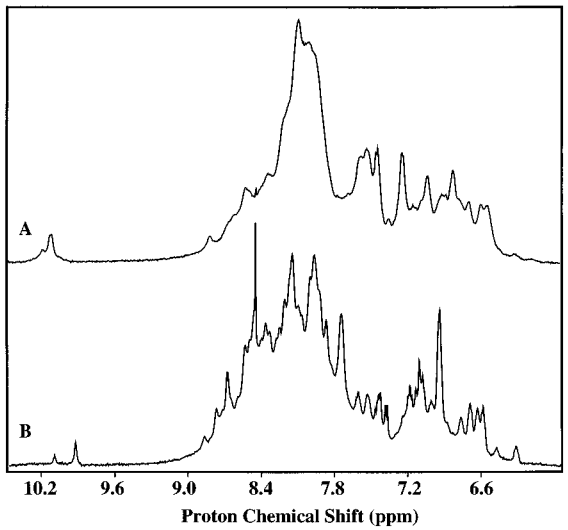

FIGURE 9: One-dimensional NMR spectra of the (A) prototype apo-H10H24 and (B) $[\alpha_2]_2$ molecules. Apo-H10H24 and $[\alpha_2]_2$ concentrations were 500 and 250 μM four-helix bundle, respectively. Spectra were acquired using identical acquisition and processing parameters with the exception that the H10H24 spectrum is signal-averaged from 256 scans and $[\alpha_2]_2$ from 1024 scans.

NMR Spectroscopy. Figure 9 shows the one-dimensional proton NMR spectra of the apo form of the prototype heme protein maquette, H10H24 (Robertson et al., 1994), which exhibits relatively poor chemical shift dispersion and large line widths for the amide and aromatic protons. In contrast, the NMR spectrum of $[\alpha_2]_2$ displays relatively good amide and aromatic proton chemical shift dispersion approaching those observed for small globular proteins. This suggests $[\alpha_2]_2$ exists in a narrow range of conformations approaching singularity in solution, whereas H10H24 is either adopting many different thermally accessible conformations that are slowly interconverting on the proton chemical shift time scale or forming nonspecific aggregates at high concentration. However, the latter possibility appears remote since the NMR spectrum of H10H24 does not change in the concentration range of 15−500 μM. Furthermore, comparison of the ^{1}H−^{1}H COSY spectra for $[\alpha_2]_2$ and a structurally well-defined variant of H10H24 (H10H24-L6I,L13F) are quite similar (B. R. Gibney, unpublished data), further supporting our view that $[\alpha_2]_2$ is nativelike.

Stable secondary, tertiary, and quaternary structures protect amide protons from exchange with solvent (Englander & Kallenbach, 1984). Numerous amide protons were observed after dissolving $[\alpha_2]_2$ in D_2O at pD 8.05 and 32 °C. Under these solution conditions the calculated exchange rate constants for random coil $[\alpha_2]_2$ amide protons range from 2.5×10^3 to 2×10^5 min^{-1} (Bai et al., 1993, 1994). While many protons completely exchanged within the first 30 min of dissolving the protein in D_2O, ~30% of the protons displayed protection factors of 10^3−10^6 and the exchange rate for the slowest exchanging amide proton in $[\alpha_2]_2$ was attenuated by a factor of 4.0×10^6. This range of protection factors extending from quite small to 10^8 is comparable to amide exchange properties observed in small globular proteins such as cytochrome *c* (Wand et al., 1986).

DISCUSSION

A four helix bundle, $[\alpha_2]_2$, related to our heme protein maquettes but with the histidine ligands removed and a site-

directed spin-label and a pendant coproporphyrin added, has been utilized to investigate the stability, topology, and dynamics of our basic four helix bundle scaffold. The 62 amino acid peptides, designed as helix−loop−helix monomers, [α_2], that would dimerize in solution, were proven to be the expected [α_2]$_2$ dimers by gel-permeation chromatography and ESR spectroscopy. Circular dichroism, FTIR, and NMR spectroscopies showed [α_2]$_2$ to be a highly helical and a nearly nativelike four helix bundle that is remarkably stable with respect to denaturants (ΔG^{H_2O} > 25 kcal/mol). The denaturation curves of the five peptides derived from three different spectroscopic techniques are presented in Figure 8. While these data show some hysteresis due to the evaluation of five slightly different peptides of very high stability, they demonstrate that the incorporation of either the nitroxide spin-label, the pendant coproporphyrin, or both has a relatively minor effect, within the ±2 kcal/mol experimental error, on the global stability of the bundle.

The stability of the 124-residue [α_2]$_2$ ([Gdn·HCl]$_{1/2}$ = 6.7 M; ΔG^{H_2O} = 25.7 kcal mol^{-1}; m = 2.7 kcal mol^{-1} M^{-1}) is comparable to the 74-residue [α_4] of DeGrado ([Gdn·HCl]$_{1/2}$ = 6.3 M, ΔG^{H_2O} = 22.5 kcal mol^{-1}, m = 3.57 kcal mol^{-1} M^{-1}) and provides a framework of sufficient stability for the incorporation of cofactor binding sites in future studies. In this regard, it is likely that the longer helices of our [α_2]$_2$ and perhaps the helix dipole orientation compensate for any loss of stabilization caused by the absence of the third loop region present in [α_4]. In comparison to our heme-binding prototype, H10H24 ([Gdn·HCl]$_{1/2}$ = 4.7 M, ΔG^{H_2O} = 16.9 kcal mol^{-1}, m = 1.9 kcal mol^{-1} M^{-1}), [α_2]$_2$ is significantly more stable with a more cooperative unfolding transition. The basis for this may be the destabilizing presence of the four histidines in amphiphilic *a* positions in the helices of H10H24. Although incorporation of four hemes into H10H24 stabilizes the bundle with respect to denaturants, the stability remains less than in our basic scaffold, [α_2]$_2$, developed for the present studies.

The site-directed spin-label provides novel insight into the stability, dynamics and topology of the four helix bundle [MAL-6-α_2]$_2$, illustrating the utility of its addition to the methodologies used in the design of new proteins. Spin-labels follow the dynamics of their locale and are able to discriminate between several distinct conformational states of these four-helix bundles. The spin-label has enabled the determination of the rotational correlation time of the bundle [MAL-6-α_2]$_2$, corroborating the four helix bundle aggregation state determined by size-exclusion chromatography. Both of the spin-labels of [MAL-6-α_2]$_2$ reside within the hydrophobic core, inaccessible to solvent, separated by a distance of >15 Å, indicating that this bundle has an antiparallel topology, as shown in Figures 1 and 10, information normally inferred from molecular modeling (Betz & DeGrado, 1996) but only established with high confidence from direct three-dimensional structure analysis by X-ray or NMR. Disassembly of the four helix bundle into monomers by trifluoroethanol provides a more rapidly tumbling spin-label which is partially restricted by the presence of secondary structure. The most highly mobile spin-labels are observed in the guanidine hydrochloride denatured state. In addition, the spin-label exposed to solvent in [CP-MAL-6-α_2]$_2$ has a high degree of rotational freedom, thus indicating significant reorganization of the bundle to provide full solvent exposure for an amphiphilic *a* position in the hydrophobic core.

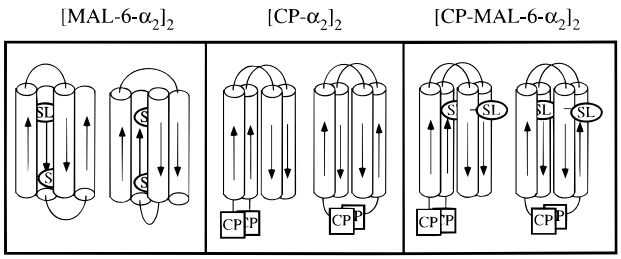

FIGURE 10: Four-helix bundle topologies consistent with the results. (Left panel) The antiparallel orientation of [MAL-6-α_2]$_2$ restricts the structure to the two topologies shown with an estimated $S_{Cys}-S_{Cys}$ distance of 27 Å. (Center and right panels) The parallel disposition of the monomers in [CP-α_2]$_2$ and [MAL-6-CP-α_2]$_2$ results in the two topologies shown with a approximate $S_{Cys}-S_{Cys}$ distance of 10 Å. The helix macrodipoles are shown as arrows for clarity.

The pendant coproporphyrin used in this study proves itself to be a very useful probe into the topology and assembly of the four-helix bundles [CP-α_2]$_2$ and [CP-MAL-6-α_2]$_2$, offering an additional methodology to apply to protein folding and design (Rabanal et al., 1996b). However, under the conditions used, the slight intrinsic tendency of the coproporphyrin to form the cofacial dimer is able to control the bundle topology by overcoming any preferences of the spin-labels or the hydrophobic core toward an antiparallel bundle. The hydrophobic packing within our basic scaffold is adequate to exclude one of the spin-labels on an interior residue to solvent upon reorientation of the monomers from antiparallel to parallel. While neither probe affects the global stability of the bundle greatly, the coproporphyrin appears to be the dominant of the two probes by controlling the topology. Dissociation of the porphyrin dimer with guanidine hydrochloride follows the denaturation of the peptide followed by CD, illustrating how the porphyrins may be used as a spectral probe of peptide dissociation and denaturation. The global stability of the bundle allows for local destabilization when the spin-label on an interior residue is exposed to solvent.

A working model for these observations is a highly stable and dynamic four helix bundle which can adopt either an antiparallel or parallel topology with a relatively small energetic barrier to interconversion, estimated from denaturation data to be less than 2 kcal/mol. The hydrophobic core is mostly composed of leucine side chains that may pack equally well regardless of helix orientation, contributing to the low height of the interconversion barrier. While in the absence of the spin-label or coproporphyrin optical probes the orientation of the parent, [α_2]$_2$, cannot be determined, the relatively well-dispersed NMR spectrum of [α_2]$_2$ and the hydrogen exchange data indicate the peptide has properties approaching those of a nativelike state that exists in a single topology. Even in this highly stable and near nativelike structure, the low interconversion barrier may be overcome by the probes without significant changes in the global stability. Clearly, while spectral probes (and cofactors) offer a ready way for determining global and local structure, their influence when examining the assembly and structure of designed synthetic proteins must be recognized. Future exact quantitation and modulation of the influence of probes (and cofactors) such as the ones presented in this report will lead to their controlled use as innocent probes and structural perturbants of protein structure.

ACKNOWLEDGMENT

Mass spectroscopic analyses were performed by the Protein Chemistry Laboratory of the University of Pennsylvania. We thank Dr. Kim Sharp for aid in preparing Figure 1.

REFERENCES

Bai, Y., Milne, J. S., Mayne, L., & Englander, S. W. (1993) *Proteins: Struct., Funct., Genet. 17*, 75.
Bai, Y., Milne, J. S., Mayne, L., & Englander, S. W. (1994) *Proteins: Struct., Funct., Genet. 20*, 4.
Berliner, L. (1972) *Biochemistry 11*, 2921.
Betz, S. F., & DeGrado, W. F. (1996) *Biochemistry 35*, 6955.
Betz, S. F., Raleigh, D. P., & DeGrado, W. F. (1993) *Curr. Opin. Struct. Biol. 3*, 601.
Bryson, J. W., Betz, S. F., Lu, H. S., Suich, D. J. Zhou, H. X., O'Neil, K. T., & DeGrado, W. F. (1995) *Science 270*, 935.
Chakrabartty, A., Kortemme, T., & Baldwin, R. L. (1994) *Protein Sci. 3* 843.
Chen, Y.-H., Yang, J. T., & Chau, K. H. (1974) *Biochemistry 13*, 3350.
Choma, C. T., Lear, J. T., Nelson, M. J., Dutton, P. L., Robertson, D. E., & DeGrado, W. F. (1994) *J. Am. Chem. Soc. 116*, 856.
DeGrado, W. F., Wasserman, Z. R., & Lear, J. T. (1989). *Science 243*, 622.
Desjarlais, J. R., & Handel, T. M. (1995) *Protein Sci. 4*, 2006.
Dill, K. A., Bromberg, S., Yue, K., Fiebig, K. M., Yee, D. P., Thomas, P. D., & Chan, H. S. (1995) *Protein Sci. 4*, 561.
Ding, H., Moser, C. C., Robertson, D. E., Tokito, M. K., Daldal, F., & Dutton, P. L. (1995) *Biochemistry 34*, 15979.
Dunback, R. L., & Karplus, M. (1994) *Nat. Struct. Biol. 1*, 334.
Englander, S. W., & Kallenbach, N. R. (1984) *Q. Rev. Biophys. 16*, 521.
Farahbakhsh, Z. T., Hideg, K., & Hubbell, W. L. (1993) *Science 262*, 1416.
Fiori, W. R., & Millhauser, G. L. (1995) *Biopolymers (Pept. Sci.) 37*, 243.
Ghadiri, M. R., & Choi, C. (1990) *J. Am. Chem. Soc. 112*, 1630.
Gibney, B. R., Mulholland, S. E., Rabanal, F., & Dutton, P. L. (1995) in *Photosynthesis: from Light to Biosphere* (Mathis, P., Ed.) Kluwer Press, Boston.
Gibney, B. R., Mulholland, S. E., Rabanal, F., & Dutton, P. L. (1996) *Proc. Natl. Acad. Sci. U.S.A.* 93, 15041.
Goldman, S. A., Bruno, G. V., Polnaszek, C. F., & Freed, J. H. (1972) *J. Chem. Phys. 56*, 716.
Goldman, S. A., Bruno, G. V., & Freed, J. H. (1973) *J. Chem. Phys. 59*, 3071.
Graddis, T. J., Myszka, D. G., & Chaiken, I. M. (1993) *Biochemistry 32*, 12664.
Handel, T. M., Williams, S. A., & DeGrado, W. F. (1993) *Science 261*, 879.
Hellinga, H. W., & Richards, F. W. (1994) *Proc. Natl. Acad. Sci. U.S.A. 91*, 5803.
Ho, S. P., & DeGrado, W. F. (1987) *J. Am. Chem. Soc. 109*, 6751.
Hubbell, W. L., & Altenbach, C. (1994) *Curr. Opin. Struct. Biol. 4*, 566.
Kalsbeck, W. A., Robertson, D. E., Pandey, R. K., Smith, K. M., Dutton, P. L., & Bocian, D. F. (1996) *Biochemistry 35*, 3429.
Kamtekar, S., Schiffer, J. M., Xiong, H., Babik, J. M., & Hecht, M. H. (1993) *Science 262*, 1680.
Klug, C. S., Su, W., Liu, J., Klebba, P. E., & Feix, J. B. (1995) *Biochemistry 34*, 14230.
Lassman, G., Ebert, B., Kuznetsov, A. N., & Damerau, W. (1973) *Biochim. Biophys. Acta 310*, 298.
Lau, S. Y. M., Taneja, A. K., & Hodges, R. S. (1984) *J. Biol. Chem. 259*, 13253.
Liu, J., Rutz, J. M., Klebba, P. E., & Feix, J. B. (1994) *Biochemistry 33*, 13274.
McGregor, M. J., Islam, S. A., & Sternberg, M. J. E. (1987) *J. Mol. Biol. 198*, 295.
Mchaourab, H. S., Hyde, J. S., & Feix, J. B. (1993) *Biochemistry 32*, 11895.
Mchaourab, H. S., Lietzow, M. A., Hideg, K., & Hubbell, W. L. (1996) *Biochemistry 35*, 7692.
Miich, S. M., Martinez, G. V., Fiori, W. R., Todd, A. P., & Millhauser, G. L. (1992) *Nature 359*, 653.
Millhauser, G. L., Fiori, W. R., & Miich, S. M. (1995) *Methods Enzymol. 246*, 589.
Mok, Y.-K., De Prat Gay, G., Butler, P. J., & Bycroft, M. (1996) *Protein Sci. 5*, 310.
Morrisett, J. D., & Broomfield, C. A. (1971) *J. Am. Chem. Soc. 93*, 7297.
O'Neil, K. T., & DeGrado, W. F. (1990) *Science 250*, 646.
Pace, C. N. (1986) *Methods Enzymol. 131*, 266.
Rabanal, F., DeGrado, W. F., & Dutton, P. L. (1996a) *J. Am. Chem. Soc. 118*, 473.
Rabanal, F., DeGrado, W. F., & Dutton, P. L. (1996b) *Tetrahedron Lett. 37*, 1347.
Rabanal, F., Gibney, B. R., DeGrado, W. F., Moser, C. C, & Dutton, P. L. (1996c) *Inorg. Chim Acta. 243*, 213.
Regan, L., & Clarke, N. D. (1990) *Biochemistry 29*, 10878.
Resek, J. F., Farahbakhsh, Z. T., Hubbell, W. L., & Khorana, H. G. (1993) *Biochemistry 32*, 12025.
Robertson, D. E., Farid, R. S., Moser, C. C., Urbauer, J. L., Mulholland, S. E., Pidikiti, R., Lear, J. L., Wand, A. J., DeGrado, W. F., & Dutton, P. L. (1994) *Nature 368*, 425.
Schneider, D. J., & Freed, J. H. (1989) in *Biological Magnetic Resonance*, Plenum, New York.
Singh, R. J., Feix, J. B., Mchaourah, H. S., Hogg, N., & Kalyanaraman, B. (1995) *Arch. Biochem. Biophys. 320*, 155.
Smith, C. K., & Regan, L. (1995) *Science 270*, 980.
Smythe, M. L., Nakaie, C. R., & Marshall, G. R. (1995) *J. Am. Chem. Soc. 117*, 10555.
Snel, M. M. E., & Marsh, D. (1993) *Biochim. Biophys. Acta 1150*, 155.
Snel, M. M. E., de Kruijff, B., & Marsh, D.(1994) *Biochemistry 33*, 11150.
Struthers, M. D., Cheng, R. P., & Imperiali, B. (1996) *Science 271*, 342−344.
Trumpower, B. L. (1990) *J. Biol. Chem. 265*, 11409.
Voss, J., Hubbell, W. L., & Kaback, H. R. (1995a) *Proc. Natl. Acad. Sci. U.S.A. 92*, 12300.
Voss, J., Salwinski, L., Kaback, H. R., & Hubbell, W. L. (1995b) *Proc. Natl. Acad. Sci. U.S.A. 92*, 12295.
Wade, W. S., Koh, J. S., Han, N., Hoekstra, D. M., & Lerner, R. A. (1993) *J. Am. Chem. Soc. 115*, 4449.
Wand, A. J., Roder, H., & Englander, S. W. (1986) *Biochemistry 25*, 1107.
Zhou, N. E., Kay, C. M., & Hodges, R. S. (1992) *J. Biol. Chem. 267*, 2664.
Zhou, N. E., Kay, C. M., Sykes, B. D., & Hodges, R. S. (1993) *Biochemistry 32*, 6190.

BI9618225